

1 **Experimental Study of the Moisture Susceptibility and Fatigue Performance**
2 **of Hydrated Lime Modified Asphalt Concrete and a Design Application Case**
3 **Study**

4
5 ^{1,3}Ahmed F. Al-Tameemi, ¹Yu Wang*, ²Amjad Albayati, ¹Jonathan Haynes

6 1. School of Computing, Science & Engineering, University of Salford, Manchester UK

7 2. Department of Civil Engineering, University of Baghdad, Iraq

8 3. Department of Civil Engineering, Al-Nahrain University, Baghdad, Iraq
9

10 **ABSTRACT**

11 Hydrated lime has been recognized as an effective additive used to improve asphalt concrete
12 properties in pavement applications. However, further work is still needed to quantify the effect of
13 hydrated lime on asphaltic concrete performance under varied weather, temperature and
14 environmental conditions and in the application of different pavement courses. A research project
15 has been conducted using hydrated lime to modify the asphalt concretes used for the applications
16 of wearing (surface), levelling (binder) and base courses. A previous publication has reported the
17 experimental study on the resistance to Marshall stability and the volumetric properties, the
18 resilient modulus and permanent deformation at three different weather temperatures. This paper
19 reports the second phase experimental study for material durability, which investigated the effect
20 of hydrated lime content on moisture susceptibility when exposed to a freeze-thaw cycle, and the
21 fatigue life. The experimental results show an improvement in the durability of the modified
22 asphalt concrete mixtures. Optimum hydrated lime contents for different course applications are
23 suggested based on the series experimental studies. Finally, the advantage of using the optimum
24 mixtures for a pavement application is demonstrated.
25

26 **Keywords**

27 Asphalt concrete, Hydrated lime, Durability, Moisture susceptibility, Fatigue life, Pavement
28 design.
29

30 *Corresponding Author, Email: y.wang@salford.ac.uk

INTRODUCTION

32
33
34
35
36
37
38
39
40
41
42
43
44
45
46
47
48
49
50
51
52
53
54
55
56
57
58
59
60
61
62

Moisture damage, fatigue cracking and accumulated permanent deformation (rutting) are the three major distresses in the property deterioration and the reduction in durability of flexible pavements. To address these problems, hydrated lime (Ca(OH)_2) has proven to be an effective additive, able to improve the mechanical properties and durability of asphalt concrete in pavement applications (Lesueur et al. 2016). Previous studies have found that asphalt concretes with added hydrated lime, which is normally used as a partial substitute for the conventional filler, limestone, showed a reduction in hardening age; an increase of flexural stiffness and resilient modulus at moderate and high temperatures; and improved ability to resist permanent deformation (Sebaaly et. al. 2001, Little et al. 2006, Albayati 2012, Albayati and Ahmed 2013). Hydrated lime displays a significant effect on the volumetric properties of concrete mixtures. A high hydrated lime content corresponds to a high asphalt content for mixtures of optimum properties (Albayati 2012). This means that the use of hydrated lime has less influence on the quantity of the main binder component of asphalt concrete. Compared with other conventional mineral fillers, such as fly ash and phosphogypsum, hydrated lime showed greater improvement in stiffness and rutting resistance of the modified asphalt concrete (Al-Suhaibani et al. 1992; Satyakumar et al. 2013).

When moisture is present in asphalt concrete it causes loss of strength and stiffness through a progressive process. The propagation of moisture damage generally occurs by two main mechanisms: loss of adhesion (stripping) and loss of cohesion (softening). Loss of adhesion happens at the interface between the aggregate and asphalt binder, while the loss of cohesion happens inside the matrix of the asphalt binder (mastic). Both laboratory and field studies have confirmed that hydrated lime is effective in controlling moisture damage for asphalt concrete (Al-Qadi et al. 2014). Hydrated lime has also proven to be effective to improve general mechanical properties, including fracture strength and fatigue life, of rubber modified hot asphalt mixtures at a hot weather temperature of 35°C (Othman 2011). The particle size plays an important role in the effect of hydrated lime on asphalt binder mechanisms. A study of the rheological characteristics of the foamed warm mix asphalt indicated that nano-sized hydrated lime modified asphalt binders exhibited a lower rutting potential. However, regular-sized hydrated lime modified asphalt binder presented a lower possibility to fatigue cracking (Diab and You, 2014).

63 Hydrated lime has a high Rigden air void value or high porosity at both dry and compacted states,
64 which is nearly twice that of conventional mineral fillers (Lesueur et al. 2013). It also has a very
65 high specific surface area, which is nearly ten times that of the conventional mineral fillers. The
66 stiffening effect of hydrated lime may be partially explained by its high Rigden air void value and
67 specific surface area, because high specific surface area increases the contact of hydrated lime
68 particles with asphalt cement particles. Additionally, hydrated lime is an active filler, which
69 precipitates the calcium ions on aggregate surfaces. The high content of calcium ions helps to
70 create a chemical bond between silica in the aggregate and the acidic radical composition in
71 bitumen in the form of water-insoluble salts (Ishai & Craus, 1977). It consequently improves the
72 bitumen–aggregate adhesion (Blazek et al. 2000). Hydrated lime also slows down bitumen ageing
73 because of the acid–base reactions between hydrated lime and the acids naturally present in the
74 bitumen (Little & Petersen, 2005).

75

76 Hydrated lime has been reported upon in general for antistrip purposes in its pavement wearing
77 surface application and at the range just up to 2% of the total asphalt concrete weight
78 (EuLA_EN_2011_12_28). So far, using hydrated lime for other pavement layer application and
79 the behaviour at varied temperature conditions have been little reported. The use of hydrated lime
80 to modify asphalt concrete used for the whole pavement structure still faces insufficient knowledge
81 from laboratory experiments and field tests. For this reason, extensive studies of the major
82 mechanical behaviours of asphalt concrete are still required in order to understand how to quantify
83 the usage of hydrated lime for the applications of different purposes and under varied
84 environmental conditions. In an effort to enrich our knowledge in this aspect, a systematic research
85 has recently been conducted using hydrated lime to modify the asphalt concrete mixtures intended
86 for the application of three types of pavement course, i.e., wearing (or surface), levelling (or
87 binder) and base at varied temperature conditions. A previous publication (Al-Tameemi et al.,
88 2016) has reported the 1st phase work, the experimental study on the volumetric and Marshall
89 properties, resistance to permanent deformation and the resilient modulus of hydrated lime
90 modified mixtures under three temperatures. The experimental results suggested that an optimum
91 2.5% replacement of conventional lime stone filler using hydrated lime should be adopted in
92 practice for all applications and weather conditions. This paper reports the 2nd phase of the
93 research, the experimental study of the moisture susceptibility and fatigue performance of the

94 modified mixtures. Finally, a case study has been investigated using the optimum mixtures for a
95 pavement structure design and predicts effectiveness for real world applications.

96

97

EXPERIMENTS

98 **Raw Materials and Mixture**

99 The component materials used in this research were asphalt cement of 40-50mm penetration grade,
100 aggregates, and mineral fillers (limestone dust and hydrated lime). The raw material properties
101 have been reported in a previous paper (Al-Tameemi *et al.* 2016). Control mixes at first were
102 prepared using limestone dust as the only mineral filler at the proportion of 7%, 6% and 5% by the
103 total weight of the aggregate for the mixes used for wearing, levelling and base course applications,
104 respectively. Meanwhile, referring to the control mix, other modified mixes were prepared using
105 hydrated lime to replace the limestone dust filler at five different rates, they are 1.0, 1.5, 2.0, 2.5
106 and 3.0% by the total weight of the aggregates. Hydrated lime was added to the mixtures in the
107 dry state. Table 1 gives the mix designs. Table 2 shows the particle size distribution of the
108 aggregates and mineral fillers together against the specification defined in SCRB/R9 (2003).

109

110 **Experimental Procedure**

111 For the designed mixtures in Table 1, at first, the Marshall stability and flow tests were conducted
112 to obtain the optimum asphalt content for the control and hydrated lime modified mixes in terms
113 of the required stability, air void content and density. Thereafter specimens were prepared, which
114 took the determined optimum asphalt content, and tested for moisture susceptibility and fatigue
115 life.

116

117 **Optimum Asphalt Content (OAC)**

118 The Marshall stability and flow tests followed the Marshall method summarized in the manual
119 series No. 2 produced by Asphalt Institute (1984). The asphalt cement (without mineral filler),
120 taking percentages of the total weight of the mixtures, were in the range of 4.3~5.5 for the wearing
121 course, 4.0~5.2 for the levelling course, and 3.7~4.9 for the base course, respectively. Different
122 mixes were prepared at an interval of 0.3% in each range.

123

124 In accordance with the standards ASTM-D6926-10 (2010) and ASTM-D-1559 (2004), three
125 cylindrical specimens of the size of 101.6 mm in diameter and 63.5 mm in length were made for
126 the mixes each. These specimens were cured for 1/2 to 3/4 hours in a water bath at 60°C, after
127 which they were compression tested across the diameter at a constant loading rate of 50.8mm/min
128 (or 2 inch/min) until failure.

129

130 The test results were plotted in terms of the percentage of asphalt (by total weight of the mix) on
131 a linear scale. Each point shown on subsequent graphs is an average result of the tests of the three
132 specimens of a specific mixture. Thereafter, the Optimum Asphalt Content (OAC) was determined
133 by taking the average of the three asphalt contents of the mixtures of the same hydrated lime
134 content and respectively meeting the three criteria below:

- 135 • The maximum unit weight (density)
- 136 • The maximum stability
- 137 • 4% air voids.

138

139 **Moisture Susceptibility Test**

140 The test followed the ASTM standard (ASTM-D4867/D4867M-09). For each mix, six
141 specimens of 101.6 mm diameter × 63.5 mm in length were cast according to the optimum asphalt
142 content. Using the Marshall method, the cast specimens were compacted on both cylindrical ends
143 to achieve a targeted $7.0 \pm 0.5\%$ air void content, aiming to accelerate the laboratory moisture
144 damage test. The six specimens of each mix were thereafter divided into two sets, which were
145 tested later, respectively, under unconditioned (dry) and conditioned (saturated) states (Fig. 1(a)).

146

147 For the unconditioned state test, specimens were placed in a water bath for one hour at 25 °C.
148 Thereafter, they were taken out and surface dried with a towel prior to being tested for ultimate
149 indirect tensile strength using the splitting method (Fig. 1(b)). The load was applied at a constant
150 deformation rate of 50.8mm/minute across the cylinder diameter, via two rigid steel plates. The
151 ultimate value of the applied load was recorded and the indirect tensile strength was calculated
152 using Eq. (1) as defined by Neville & Brooks (1987).

153

$$154 \quad S_t = \frac{2P}{\pi LD} \quad (1)$$

155

156 where S_t is the tensile strength; P is the maximum load applied; L is length of the specimen and D
157 is the diameter.

158

159 For the conditioned state test, the specimens were put in a flask filled with water at an approximate
160 temperature of 25 °C. A vacuum of 70kPa or 525mmHg was applied for 5 minutes to achieve a
161 desired saturation level in the range of 70~80% in terms of the specifications in both the ASTM
162 D4867 and the modified AASHTO T283 in 2003. Thereafter, each specimen was wrapped using
163 a plastic film and sealed using tape. These wrapped specimens were transferred in airtight plastic
164 bags containing approximately 3 ml distilled water in each bag and sealed again using tape. These
165 bagged specimens were then placed in a freezer for 16 hours under a controlled temperature of -
166 18 °C. After removal from the freezer, the bagged specimens were immediately immersed in a
167 water bath of 60°C for 24 hours. Then all specimens were removed from the plastic bags and
168 wraps, and placed in another water bath at 25 °C for one hour. Thereafter, specimens were taken
169 out and dried using a towel, and then tested the indirect tensile strength following the same
170 procedure described for the unconditioned state test. For the sake of comparison, a parameter called
171 tensile strength ratio (TSR) is defined for each mix using Eq. (2).

172

$$173 \quad \text{TSR} = \frac{S_{tm}}{S_{td}} \times 100 \quad (2)$$

174

175 were, S_{tm} is the conditioned tensile strength and S_{td} is the unconditioned tensile strength.

176

177 **Fatigue Test**

178 The fatigue life test used the four point bending method (Fig. 1 (c) and (d)) which produces a pure
179 constant bending in the section of the beam between the two applied loads (Fig. 2(a)). Repeated
180 loads were applied until the failure of the beam and the maximum number of repeated load cycles
181 was taken as the fatigue life of the each mixture. A stress controlled fatigue test method, rather
182 than the strain-controlled test specified by AASHTO T321, was adopted because the available
183 pneumatic loading system was only able to provide a stress-control function. Four load levels were
184 applied by vertical downward (push) force P for each mixture, being 223, 310, 402 and 490 N.

185 Each load was applied in a rectangular repeated form with 0.1 seconds of loading followed by 0.4
186 seconds of resting (no loading) as illustrated in Fig. 2(b). There were three specimens prepared for
187 each mix and tested. The final result for each mix took the average of the three. Each specimen
188 was put in the test chamber at a controlled temperature of 20 ± 1 °C for six hours before the test to
189 allow an even temperature distribution within the specimen to develop before conducting the test.
190 A digital camera was used to record the failure process occurring at the mid-span of the beam
191 during testing. The vertical deflection of the beam at mid-span was measured using a Linear
192 Variable Displacement Transducer (LVDT) installed and connected to a data acquisition system.
193 The specimen beams had dimensions of 76mm \times 76 mm \times 381 mm. The failure of the beam was
194 taken when the specimen broke (completely split into two parts). In each test, an initial tensile
195 strain was determined at the 200th repetition in terms of Eq. (3).

$$\epsilon_t = \frac{12h\Delta}{3L^2 - 4a^2} \quad (3),$$

198
199 where ϵ_t is the tensile strain; h is height of the beam; Δ is the deflection at the centre of the beam;
200 L is the length of span between two supports; a is the distance from support to the load point ($L/3$).
201 The relation of the initial strain versus the maximum number of repetitions to failure was plotted
202 as the result.

203



204

205

(a) Specimens for splitting tensile test

(b) Indirect splitting tensile test



206

(c) Specimens for fatigue test

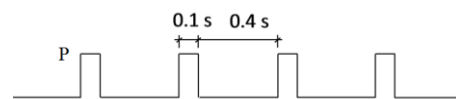
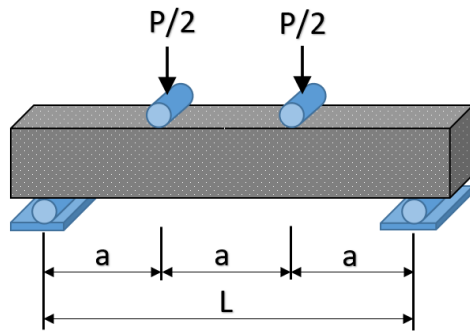
(d) Fatigue test

207

208

Figure 1. The specimens and experimental setup

209



210

(a) The four point bending flexure test

(b) The applied repeated load

211

212

Figure 2. The principle for fatigue test

213

214

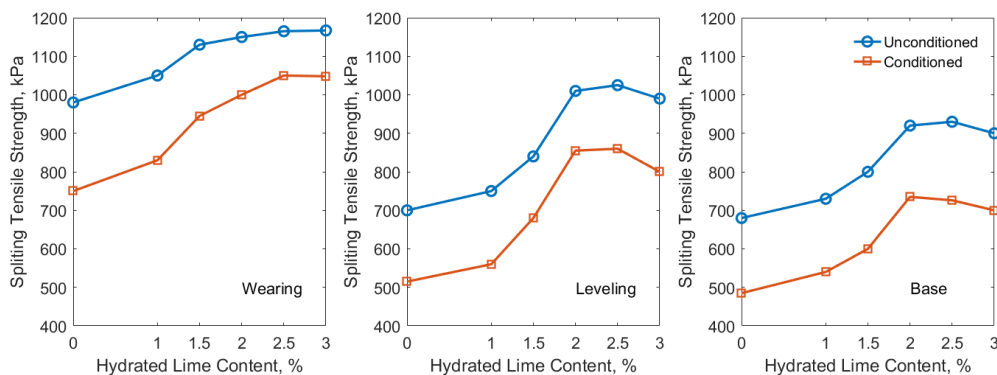
RESULTS AND DISCUSSION

Moisture Susceptibility

215 Figure 3 shows the splitting tensile strength results of the mixtures for three pavement structure

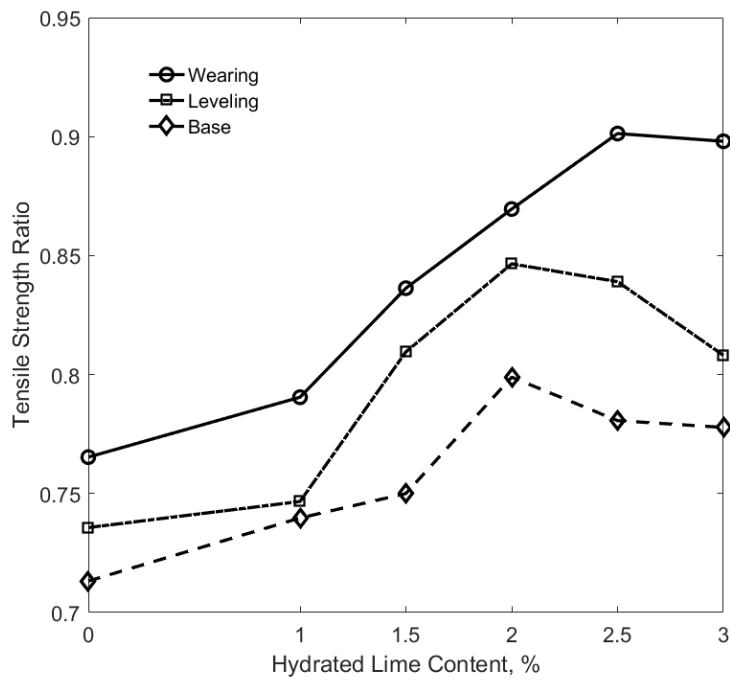
216 courses, under the unconditioned and conditioned states. Fig. 4 shows the effect of hydrated lime

218 addition on the splitting tensile strength ratio. Fig. 5 shows the percentage improvement in the
 219 splitting tensile strength of the hydrated lime modified mixtures against that of the control mix.
 220 From these results it can be seen that in general 2.5% hydrated lime content gives the optimum
 221 improvement for all the three pavement course mixtures at both unconditioned and conditioned
 222 states. Although the improvement for the unconditioned state is better than that for the conditioned
 223 state, the influence of the hydrated lime on the tensile strength ratio is not significant with a
 224 variation range of less than 0.15 (Fig. 4). Fig. 5 shows that the improvement for the unconditional
 225 state is in the range of 40~68% while that for the conditioned state is in the range of 18~45% at
 226 2.5% of hydrated lime content. The improvement for the mixtures used for levelling and base
 227 course are quite similar and better than the improvement for the wearing course mixture.
 228



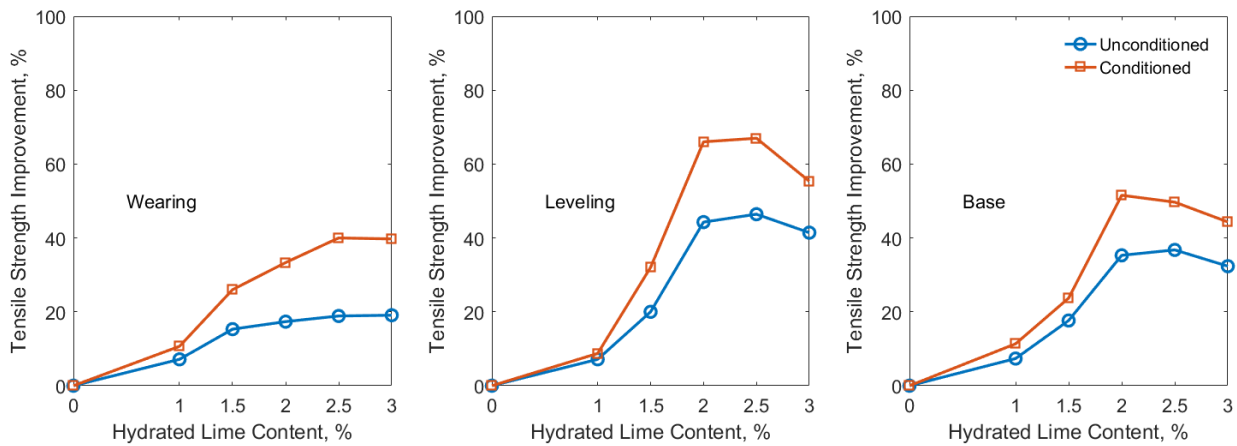
229
 230 Figure 3. Splitting tensile strength of the mixtures of different hydrated lime contents

231



232
233
234

Figure 4. The effect of hydrated lime on the tensile strength ratio (TSR)



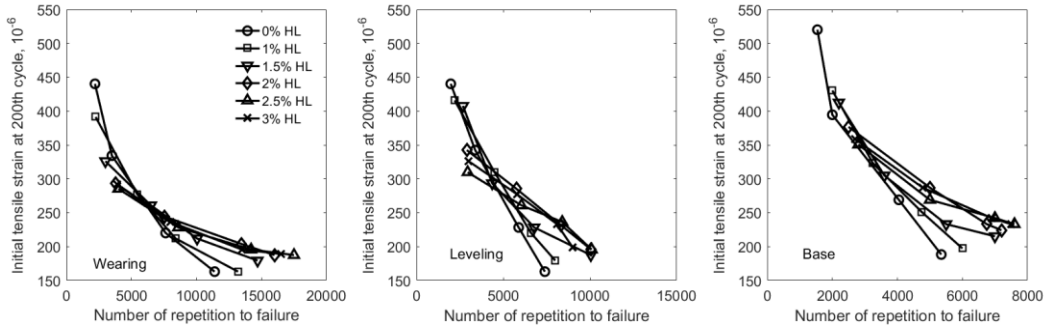
236
237
238

Figure 5. Improvement on the splitting tensile strength

Fatigue Life

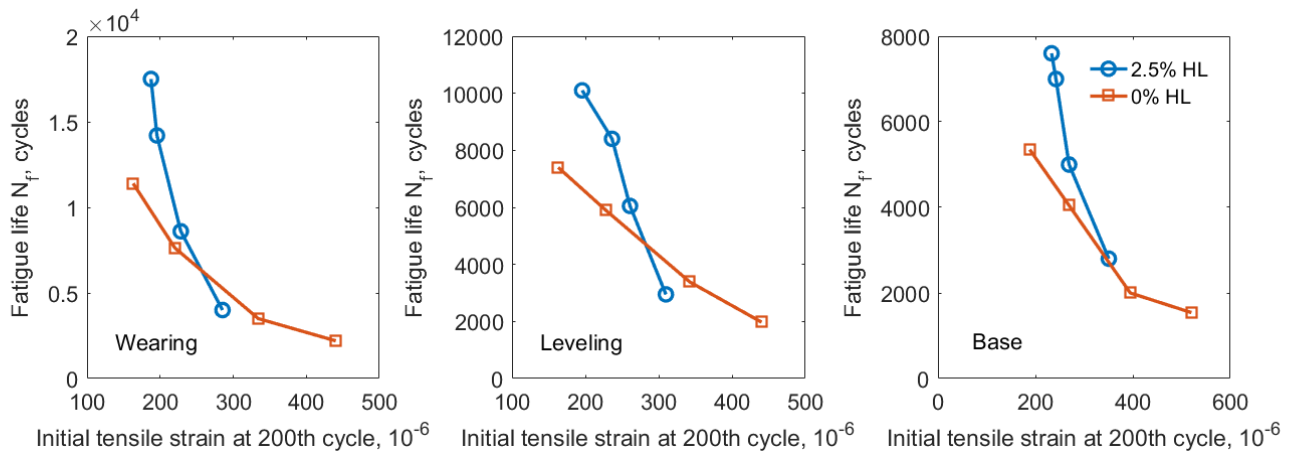
239 Figure 6 shows the relationship between the defined initial tensile strain ($\epsilon_{i,200th}$) and the maximum
240 number of load repetitions (N_f) up to failure of the beam tested, for the three pavement courses.
241 The results show that in general, the 2.5% hydrated lime (HL) content produced the maximum
242 fatigue life time for all three layer applications, and with the most significant improvement in the

243 case of the wearing course mixture. 3% HL is comparable to the 2.5% HL for the Base mix, but
 244 shows less fatigue life used for Wearing and Leveling mixes, particularly at smaller initial strain
 245 or lower load conditions.
 246

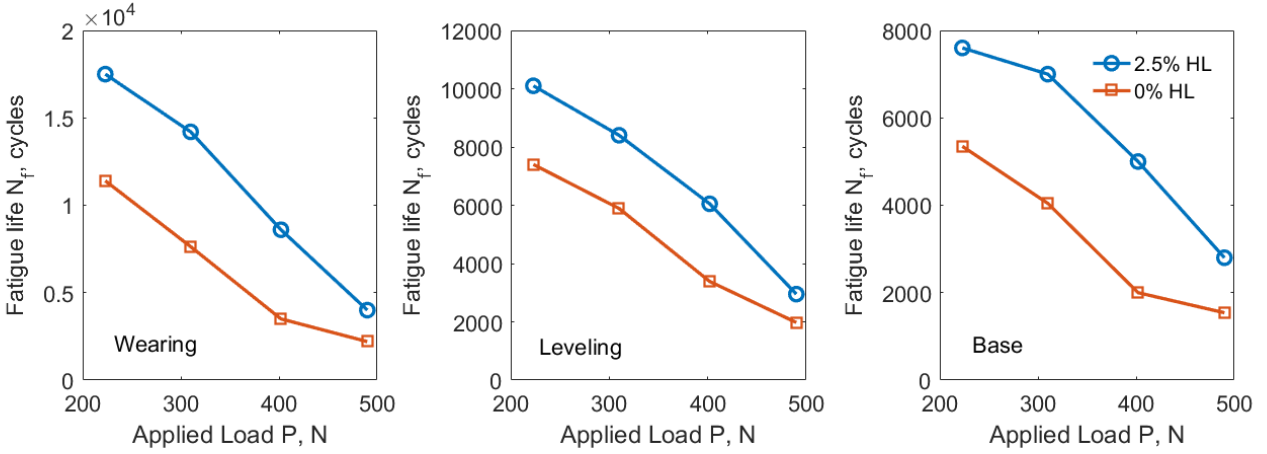


247
 248 Figure 6. Relation between initial tensile strain and the number of load repetition to failure
 249

250 The data for the control and 2.5% HL mixes content are extracted from Fig. 6 and replotted as Fig.
 251 7, showing the fatigue life at different initial strains for the three application courses. It can be seen
 252 that the optimum modified mixtures are more rigid than the control mixtures. The strain increases
 253 after an initial 200 repetitions is less than approximately 100 microstrain for all these mixtures.
 254 Fig. 8 replots the Fig. 7 data in terms of the applied loads. It clearly shows that improvement in
 255 the fatigue life is significant for all the three mixtures.
 256



258 Figure 7. Fatigue life comparison of the modified mixture with 2.5% hydrated lime in terms of
 259 the initial strain
 260



262 Figure 8. Fatigue life comparison of the modified mixture with 2.5% hydrated lime in terms of
 263 the applied load
 264

265 For the sake of pavement structural design, a power function in the form of Eq. (4) is used to
 266 characterize the deformation and fatigue life relationship, i.e., the $\epsilon_{t_{200th}}$ vs N_f curves. Fig. 9 shows
 267 the results using Eq. (4) to fit the data from Fig. 6. The data present an almost linear relationship
 268 in a log-log graph.

269

$$270 \quad \epsilon_{t_{200th}} = k_1(N_f)^{-k_2} \quad (4)$$

271

272 where k_1 and k_2 are two constants.

273

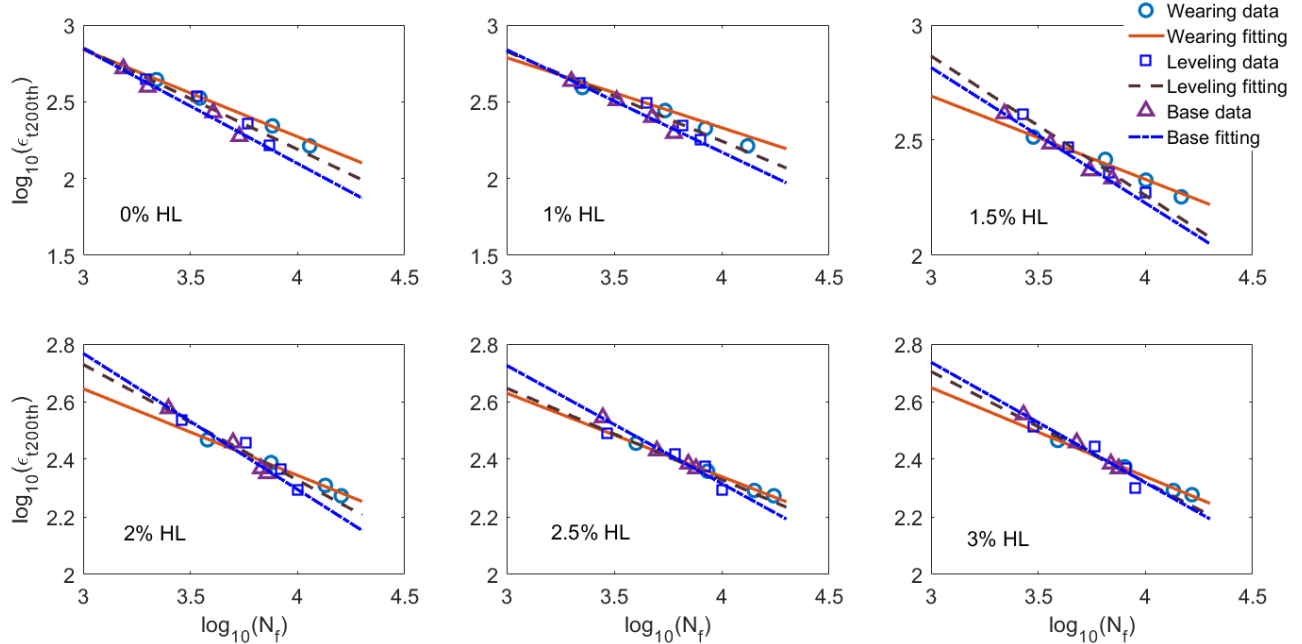
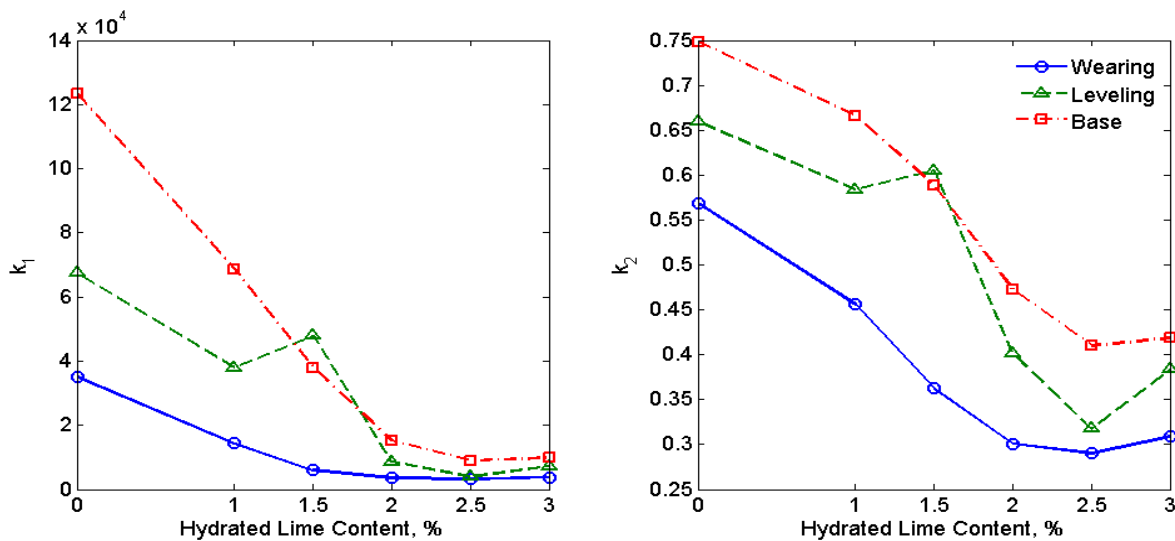


Figure 9. The characterized $\epsilon_{t,200th}$ vs N_f relation

275
276
277
278
279
280
281
282

For the relationships shown in Fig. 9, the two parameters, k_1 and k_2 , define the interception and the slope, which relate to the initial tensile strain and the rigidity under repeated loading, respectively. Fig. 10 shows the variation of k_1 and k_2 in terms of the hydrated lime content. It can be seen that the two constants are minimised at the 2.5% hydrated lime content, for all three application mixtures, which correspond to the smallest initial deformation and highest stability and rigidity.



283

284 Figure 10. The variation of k_1 and k_2 with hydrated lime content

285

286 Together with the results of the resilient modulus, permanent deformation (rutting) (Al-Tameemi
287 et al. 2016) and moisture susceptibility, it can be seen that 2.5% HL addition provides an optimum
288 result. Fundamentally, the improvement of hydrated lime addition on asphalt concrete property
289 relies on two mechanisms, i.e. the micro-void filling (hydrated lime particles themselves are
290 porous, which absorb the asphalt cement particles to form a hardened mastic phase) and the
291 enhancement of reactive surface bonding between the asphalt cement and aggregate. For a specific
292 mixture, when the total aggregate surface area is a certain constant, too much hydrated lime will
293 reduce the effective asphalt cement quantity acting as the active binder in the mix.

294

295 **A Case Study - Pavement Design Application**

296 To evaluate the benefit, this section investigates a case study using the modified asphalt concrete
297 mixtures with the optimum 2.5% hydrated lime content for a pavement structure designed for a
298 specific geological and transportation scenario.

299

300 **Application Conditions**

301 The application is set for an urban area in the City of Baghdad in Iraq, for which, with a recorded
302 annual temperature range of 4~44 °C, an average temperature 23 °C is assumed according to the
303 data published by the Iraqi Meteorological Organization and Seismology (IMOS). Much research
304 has been conducted to estimate the vertical temperature distribution profile of pavement structures
305 (Chandra et al. 1988, Diefenderfer et al 2002). In this paper, a simple model developed by Albayati
306 and Alani (2015) and recommended by the Baghdad Road Authority was adopted. The model has
307 predicted temperature profiles which prove to be comparable with other models, such as the
308 Witczak model (1972) and SHRP (Strategic Highway Research Programme 1994) model (Albayati
309 and Alani, 2015). It takes the form of Eq. (5):

310

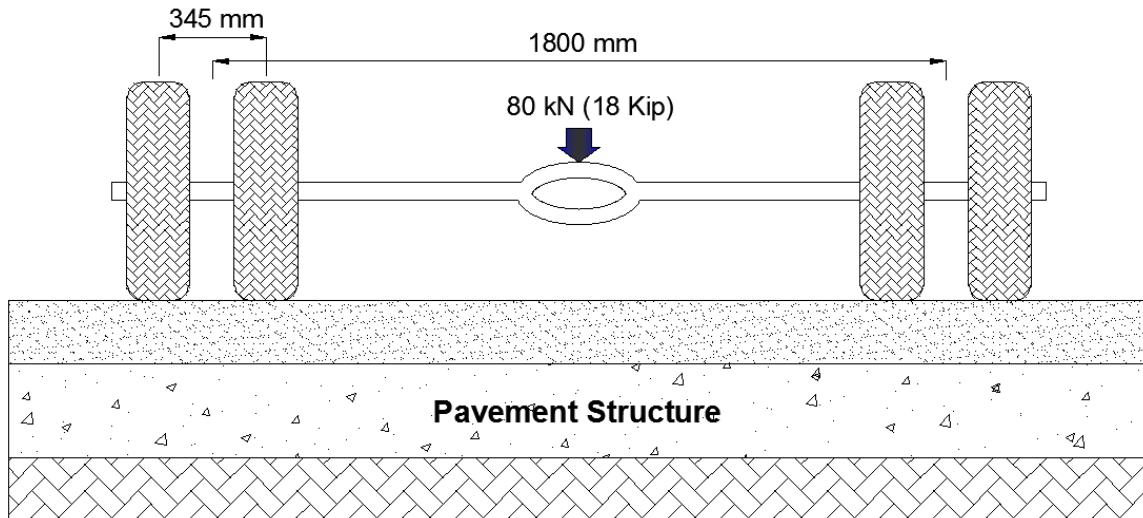
$$311 \quad T_{pave} = 1.217 \times T_{air} - 0.354 \times Z \quad (5),$$

312

313 where T_{pave} (°C) represents the temperature in pavement structure; T_{air} (°C) represents the air
314 temperature; Z (cm) is the depth in pavement below the surface.

315
316
317
318
319

Table 3 lists the estimated traffic conditions. All traffic loads are converted to an 80kN (18kip) Equivalent Single Axle Load (ESAL) as shown in Fig. 11 in accordance with the AASHTO load equivalency factors (AASHTO, 1993).



320
321
322

Figure 11. The 80 kN (18-kip) ESAL Configuration

323 Finite Element Model

324 A 3D finite element model shown in Fig. 12 was created for the pavement structure, which consists
325 of five layers, i.e., three asphalt concrete layers (wearing, levelling and base) and two foundations
326 (subbase and subgrade). The contact area between the tire and pavement surface depends on the
327 contact pressure. In terms of the suggestion by Huang (2004) the contact pressure is smaller than
328 the tire pressure for high-pressure tires (trucks), because the wall of tires is in tension. For
329 simplicity, in pavement design, the contact pressure is generally assumed to be equal to the tire
330 pressure in the consideration that the higher the axle loads, the higher tire pressures and the more
331 destructive effects on pavements (Huang, 2004). There are three contact stresses non-uniformly
332 distributed in the area (Ling et al. 2017). However, using the static vertical deformation and
333 bending tensile strain as the criteria for comparison, this study assumes a uniform vertical stress
334 in response to the traffic axle load but neglects the stress in other directions. Fig. 13(a) presents
335 the approximate shape of the contact area for each tire, which consists of a rectangle and two semi-
336 circles, where the characteristic parameter, L , is approximated to be:

337

338

$$L = \sqrt{\frac{A_c}{0.5227}} \quad (6),$$

339

340 where A_c represents the contact area between the tire and pavement, which can be acquired by

341 dividing the applied load on each tire by its pressure. The contact area illustrated in Fig. 13(a) was

342 suggested by Portland Cement Association (PCA) in 1966 for the design of rigid pavements. In

343 1984, the PCA proposed a method based on the finite element approach in which an equivalent

344 rectangular contact area was adopted. Similar to recent work by Ling et al (2017), this study uses

345 an equivalent rectangular tire imprint to represent the contact area between tire and pavement as

346 defined in Fig. 13(b). As the total load is 80 kN (18 Kip) and there are dual tires on each side of

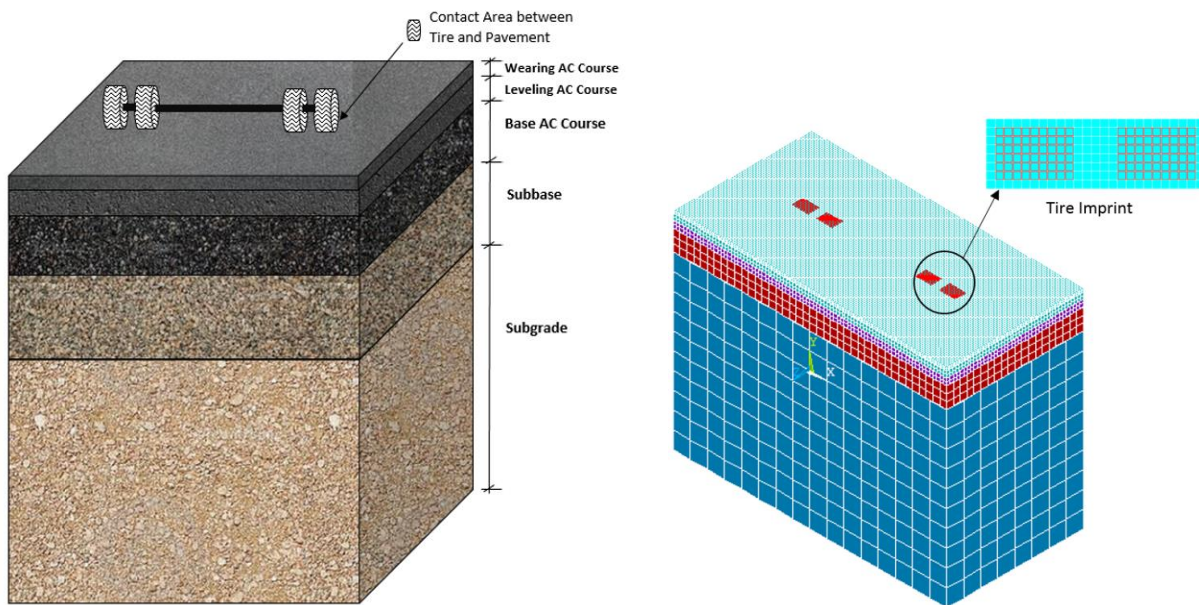
347 the axle, the load on each tire is 20 kN. The pressure of the tire is 600 kPa (87 psi). Therefore, by

348 dividing the load using the pressure, the contact area between tire and pavement is 0.03334 m².

349 Therefore, the dimensions of the rectangular equivalent area are: Length = 0.8712×0.2525 = 0.22

350 m, and Width = 0.6×0.2525 = 0.15 m

351



352

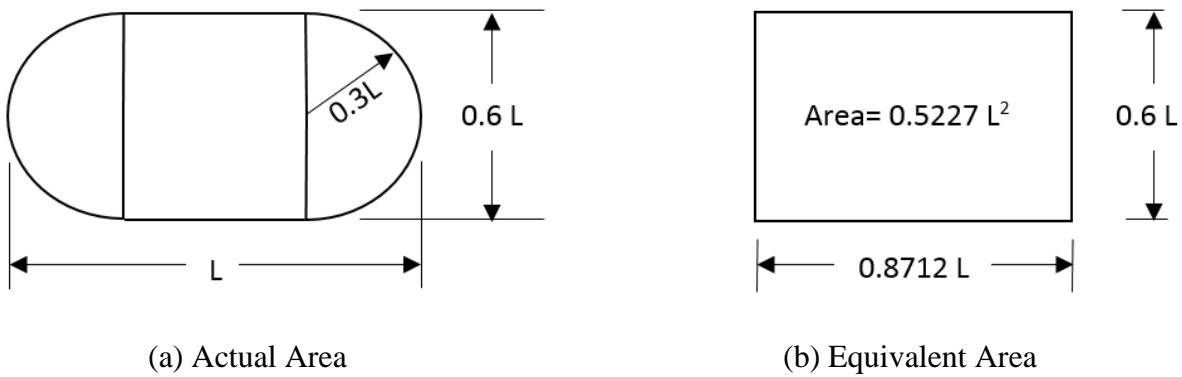
353 (a) Pavement structure

(b) FE model

354

Figure 12. Pavement structure and FE model

355



358 Figure 13. Estimation of the contact area between tire and pavement (Huang, 2004)

359

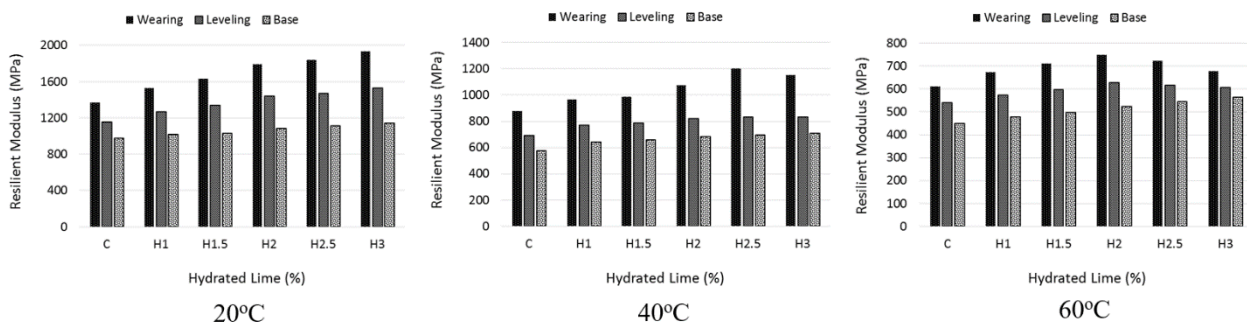
360 **Material Properties**

361 The material properties used in the FE modelling are given below.

362 • **Resilient Modulus of Asphalt Concrete Layers**

363 Figure 14 shows the measured resilient modulus of the hydrated lime modified concretes used for
 364 the three asphalt layers under three different temperatures. The work was conducted in the 1st phase
 365 of this research (Al-Tameemi et al., 2016). A simplified polynomial, i.e.: $M_r = aT_{pave}^2 + bT_{pave} + c$,
 366 is used to characterise the thermal effect on the resilient modulus, where M_r represents the resilient
 367 modulus of the modified asphalt concrete, T_{pave} is the temperature estimated using Eq. (5).

368



369

370 Figure 14. Hydrated lime influence on resilient modulus at three temperatures

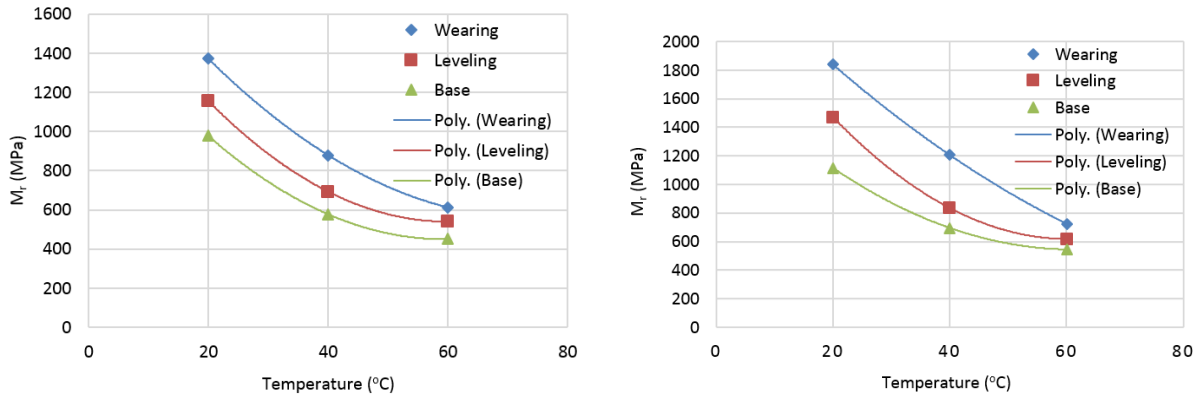
371

C – Control 0% hydrated lime, H1~H3 – 1% ~3% hydrated lime

372

373 Fig. 15 shows the modelling results using the polynomial to fit the data of the 0% and 2.5%
 374 hydrated lime in Fig. 14. Table 4 lists the corresponding three fitting parameters, a, b and c.

375



(a) Control mix of 0% hydrated lime (HL) (b) Optimum mix of 2.5% hydrated lime (HL)

Figure 15. Modelled resilient modulus of the control and modified mixtures

376

377

378

379

380 • Resilient Modulus of Subbase and Subgrade Layers

381 The models proposed by Claessen et al. (1977) at the Shell Oil Company were adopted to estimate
382 the property of these two foundation layers. For the granular subbase, its resilient modulus is
383 assumed to depend upon the property of the subgrade layer underneath, i.e.:

384

385
$$M_{r(subbase)} = K \times M_{r(subgrade)} \tag{7},$$

386

387 where $K = 0.2h^{0.45}$, and h (mm) is the thickness of the subbase layer. The K has a value in a range
388 of 2~4. The property of the subgrade layer itself is determined according to the measurement of
389 the California Bearing Ratio (CBR) following the test procedure defined in ASTM D-1883, which
390 is given below:

391

392
$$M_{R(subgrade)} = 1450CBR \tag{8},$$

393

394 where CBR is 4.5% in this study.

395

396 • Poisson Ratio

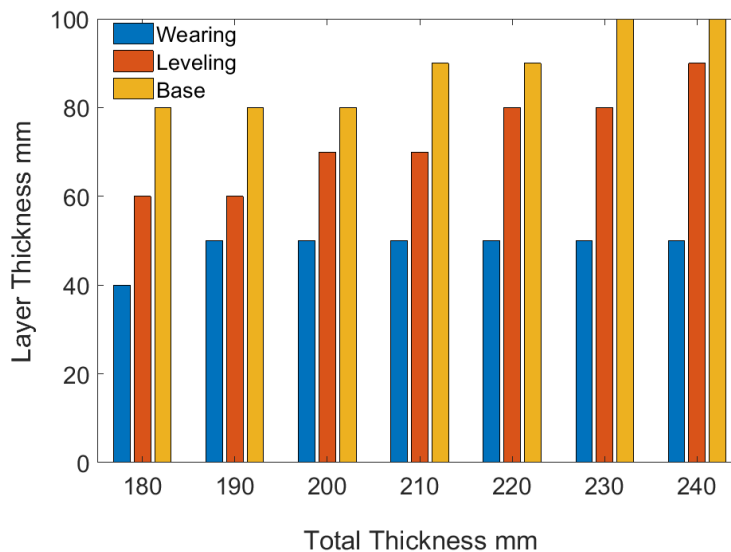
397 Poisson ratio is a fundamental property which influences the mechanical behaviour of pavement
398 structures, particularly in the analysis of deformation of pavement structures when the viscoelastic

399 material properties have to be explicitly described. In this paper, however, the pavement structure
 400 was considered as an elastic system with a relatively small deflection. In elastic range Poisson ratio
 401 variation is very small, so its influence of on stress and strain is assumed to be negligible (Huang
 402 2004). Under such conditions, the Poisson ratio is usually assumed to be a reasonable value instead
 403 of determining it from actual tests (Southgate et. al., 1977). The data listed in the Table 5 were
 404 adopted in this study.

405

406 **FEA Results and Pavement Performance Prediction**

407 The finite element analysis aims to find an optimum pavement design using the optimum
 408 hydrated lime modified concretes in comparison with using the control concretes without
 409 hydrated lime. Two different thicknesses of the wearing layer, four different thicknesses of the
 410 levelling layer and three different thicknesses of the base layer were selected. Totalling seven
 411 designs using a combination of these layer thicknesses, which give different total thicknesses of
 412 the pavement structures, were investigated. For all the cases, the subbase thickness was set as
 413 300 mm and subgrade depth was set as 2500 mm. Fig. 16 shows the seven structural designs.



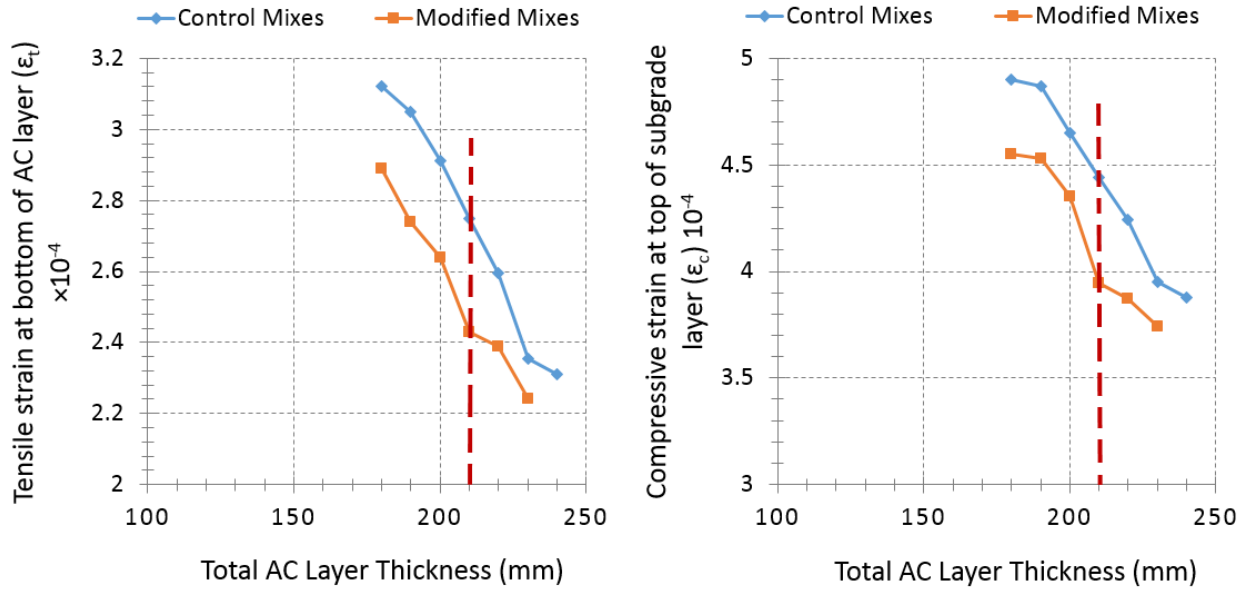
414

415 Figure 16. The pavement structure of varied thickness of the asphalt layers

416

417 Figure 17 shows a comparison of the tensile strain at the middle of the bottom of the asphalt
 418 concrete layers (bottom of the base layer), and the compressive strain at the middle of the top of

419 the subgrade. It can be seen that the optimum structure is that of a total thickness of 210 mm with
 420 50 mm of wearing, 70 mm of levelling and 90 mm of base, for which optimum hydrated lime
 421 modified mixes present the best improvement compared with using the control mixes.
 422



423
 424 Figure 17. Comparison of tensile strain and compressive strain at critical points
 425

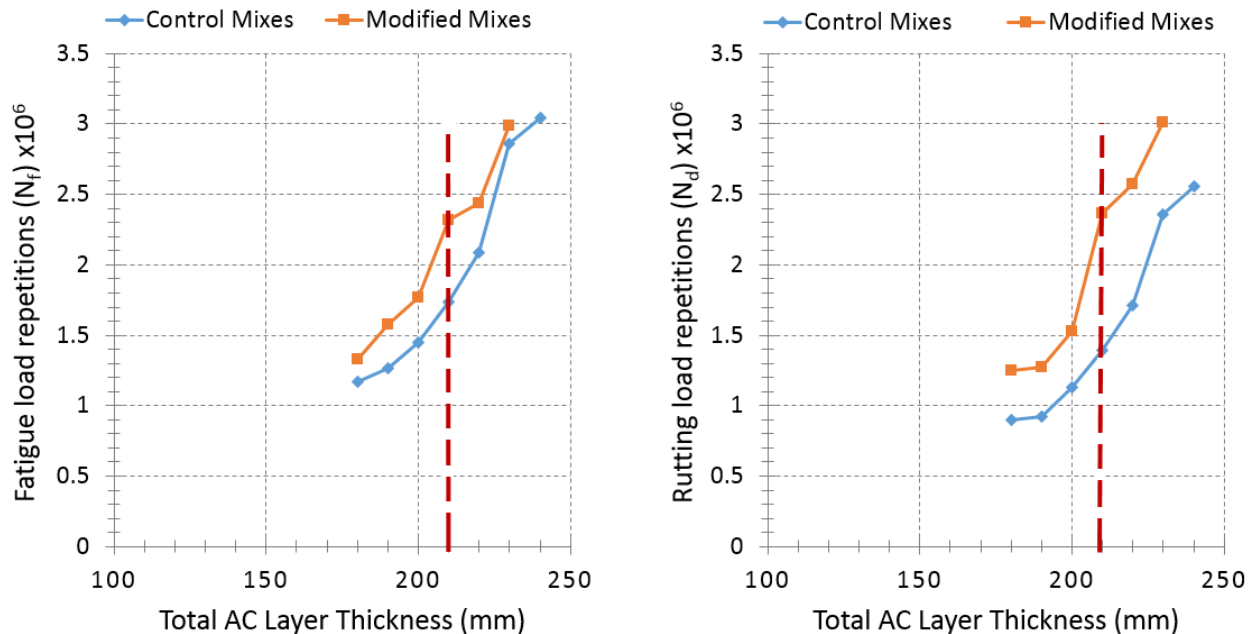
426 Base on the FEA results, Fig. 18 shows the predicted fatigue life and the maximum number of load
 427 cycles for a rutting criteria, which are estimated using two empirical models adopted in KENPAVE
 428 (Huang 2004), i.e.:

429
 430
$$N_f = 0.0796 \times \epsilon_t^{-3.291} \times M_r^{-0.854} \quad (9),$$

431
 432
$$N_d = 1.365 \times 10^{-9} \times \epsilon_c^{-4.447} \quad (10),$$

433 where N_f is the number of load repetitions to failure; ϵ_t is the horizontal tensile strain at the bottom
 434 of asphalt concrete layer, which took the maximum value of the three layers in this study; M_r is
 435 resilient modulus of asphalt concrete layer of the maximum ϵ_t ; N_d is the number of load repetition
 436 to a criteria 127 mm (0.5 inch) permanent deformation (rutting depth); ϵ_c is the vertical strain at
 437 the surface of the subgrade. It can be seen that the pavement structure of total thickness 210 mm

438 using the optimum hydrated lime modified concretes gives the best result in terms of the
 439 improvement on that using the control material under the condition to satisfy the requirement in
 440 Table 3.
 441



442
 443 Figure 18. Predicted fatigue life and permanent deformation
 444

445 Figure 19 compares the degree of improvement of all the designs using the 2.5% hydrated lime
 446 modification on that using the control material without the addition of hydrated lime, where the
 447 degree of improvement is defined as: $improvement = \frac{HL\ concrete - Control\ concrete}{Control\ concrete}$. It shows that
 448 the structure of the 210 mm total thickness provides a significant percentage improvement on both
 449 fatigue life and rutting resistance because of the enhancement of the rigidity of the hydrated lime
 450 modified concretes.

451

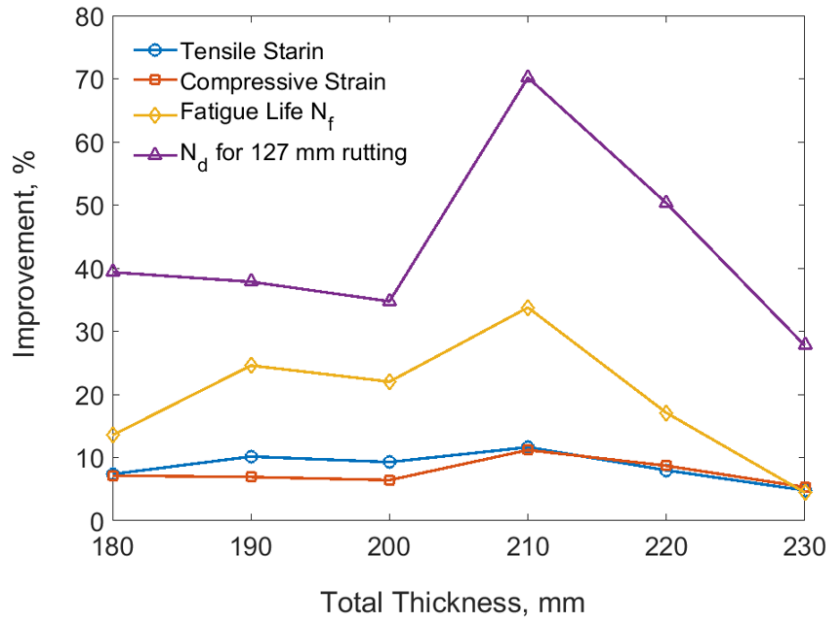


Figure 19. Improvement of structural mechanical properties and durability

CONCLUSIONS

This paper has reported an experimental study of the durability of hydrated lime modified asphalt concretes used for three different pavement courses, and a case study using the optimum mixes for a pavement design. Together with the results from previous work (Al-Tameemi et al., 2016), in which the volumetric and Marshall properties, permanent deformation and resilient modulus at various temperatures were evaluated, the follow conclusions can be drawn from this series of studies:

1. The addition of hydrated lime will enhance the mechanical properties and durability of asphalt concrete in terms of the resilient modulus, rutting resistance, moisture susceptibility under freeze-thaw conditions, and fatigue life.
2. Hydrated lime can be used not only for antistripping purposes in the mixtures for wearing course but also in the mixtures for other structural courses to produce an integration of the improvements in mechanical and durability behaviour of pavement structures.
3. The improvement of the mechanical properties works in a relatively wide range of weather temperatures.
4. A high hydrated lime content does not mean a definite improvement for the durability of mixtures because extra hydrated lime will reduce the effective amount of asphalt cement, the

472 active binder. In general, an optimum maximum of 2.5% hydrated lime content by total weight
473 of aggregate to replace the same weight of conventional mineral filler is suggested for all
474 practices in terms of both mechanical behaviour and durability improvement.

475 5. A design case study shows that using hydrated lime for all the asphalt layer courses reduces the
476 tensile strain at the bottom of the base layer and the compressive strain on the top of the
477 subgrade, and improves the total fatigue life of the whole pavement structure.

478 6. Using the mixtures of 2.5% hydrated lime addition for the three asphalt layers, an optimum
479 pavement structure in the case study has showed 30% improvement on fatigue and 70%
480 improvement on permanent deformation (rutting).

481

482 **ACKNOWLEDGEMENT**

483 Funding: This study was funded by the Iraqi Ministry of Higher Education and Scientific Research
484 Scholarship Program.

485 Conflict of Interest: The authors declare that they have no conflict of interest.

486

487 **REFERENCES**

488 Albayati, A. & Ahmed, M., 2013, Assessment of the Impact of Different Hydrated Lime Addition
489 Methods on Fatigue Life Characteristic. *Eng. & Tech. Journal*, **31**: 489-511.

490 Albayati A., 2012, Mechanistic Evaluation of Lime-Modified Asphalt Concrete Mixtures, 7th
491 RILEM International Conference on Cracking in Pavements, ed. by A. Scarpas, N. Kringos, I. Al-
492 Qadi and L. A, Springer Netherlands. **4**: 921-940.

493 Albayati, A. H. K. & Alani, A. M. M., 2015, Temperature Prediction Model for Asphalt Concrete
494 Pavement, 14th Annual International Conference on Asphalt, Pavement Engineering and
495 Infrastructure, 11th – 12th February, LJMU Liverpool, UK.

496 Al-Qadi I.L., Abuawad I.M., Dhasmana H., Coenen A.R., 2014, Effects Of Various Asphalt
497 Binder, Additives/Modifiers On Moisturesusceptible, Asphaltic Mixtures, Research Report
498 FHWA-ICT-14-004, Illinois Center for Transportation Series No. 14-004, UILU-ENG-2014-
499 2004, ISSN: 0197-9191.

500 Al-Suhaibani A., Al-Mudaiheem J. and Al-Fozan F., 1992, Effect of Filler Type and Content on
501 Properties of Asphalt Concrete Mixes, in SPT 1147 Effects of Aggregates and Mineral Fillers on
502 Asphalt Mixtures Performance, ed. By R. C. Meininger, ASTM, Philadelphia PA, 107–130.

503 Al-Tameemi A., Wang Y., Albayati A., 2016, Experimental study of the performance related
504 properties of asphalt concrete modified with hydrated lime, Journal of Material Civil Engineering,
505 **28**(5) , 04015185-1.

506 Asphalt Institute, 1984, Mix Design Methods for Asphalt Concrete and Other Hot-Mix Types.
507 Manual Series No. 2. Lexington, KY.

508 ASTM D6926-10, 2010, Standard Practice for Preparation of Bituminous Specimens Using
509 Marshall Apparatus, ASTM International, West Conshohocken, PA, USA.

510 ASTM-D-1559, 2004, Road and Paving Materials, Annual Book of ASTM Standards, Volume
511 04.03, American Society for Testing and Materials, West Conshohocken, USA.

512 ASTM-D4867/D4867M–09, The Standard Test Method for Effect of Moisture on Asphalt
513 Concrete Paving Mixtures.

514 Blazek J., Sebor G., Maxa D., Ajib M., Paniagua H., 2000, Effect of hydrated lime addition on
515 properties of asphalt. *Petroleum and Coal*, **42**(1): 41–45.

516 Chandra D, Lytton R.L., and Yang W., 1988, Effects of Temperature and Moisture on Low-
517 Volume Roads, Texas Transportation Institute Texas AIM University System.

518 Claessen, A., Edwards P., Sommer P., Uge P., 1977, Asphalt Pavement Design: The SHELL
519 Method, Proceedings 4th International Conference on The Structural Design of Asphalt
520 Pavements, University of Michigan, Ann Arbor, Michigan, USA.

521 Diab A. and You Z., 2014, Rheological Characteristics of Nano-sized Hydrated Lime-Modified
522 Foamed Warm Mix Asphalt, Pavement Materials, Structures, and Performance GSP 239 © ASCE
523 2014.

524 Diefenderfer B.K., Al-Qadi I.L., Reubush S.D., Freeman T.E., 2002, Development And Validation
525 Of A Model To Predict Pavement Temperature Profile, Research Report, Concorr Inc, Virginia
526 Tech Transportation Institute, and Virginia Transportation Research Council.

527 EuLA_EN_2011_12_28, 2011, Hydrated Lime, A Proven Additive, For Durable Asphalt
528 Pavements, critical literature review, EuLA - European Lime Association Rue des Deux Eglises
529 26, B-1000 Brussels, Belgium.

530 Huang, Y., 2004, Pavement Analysis and Design, 2nd Edition, Prentice Hall, Englewood Cliffs,
531 New Jersey, USA.

532 Ishaï I. and Craus J., 1977, Effect of the filler on aggregate-bitumen adhesion properties in
533 bituminous mixtures. *Proceedings of the Association Asphalt Paving Technologists*, **43**:228-258,
534 Lino Lakes, MN: Association Asphalt Paving Technologists (AAPT).

535 Lesueur D., Denayer C., Ritter H.-J., Kunesch C., Gasiorowski S., d'Alto A., 2016, The use of
536 hydrated lime in the formulation of asphalt mixtures: European case studies, 6th Eurasphalt &
537 Eurobitume Congress, 1-3 June 2016, Prague, Czech Republic.

538 Lesueur D., Petit J., Ritter H.-J., 2013, The mechanisms of hydrated lime modification of asphalt
539 mixtures: a state-of-the-art review, *Road Materials and Pavement Design*, **14**(1):1-16.

540 Ling, M., Luo, X., Hu, S., Gu, F., and Lytton, R. L., 2017, Numerical Modeling and Artificial
541 Neural Network for Predicting J-Integral of Top-Down Cracking in Asphalt Pavement.
542 *Transportation Research Record: Journal of the Transportation Research Board*, 2631: 83-95.

543 Little D. N. and Peterson J. C., 2005, Unique Effects of Hydrated Lime Filler on the Performance-
544 Related Properties of Asphalt Cements: Physical and Chemical Interactions Revisited, *Journal of*
545 *Materials in Civil Engineering*, **17**(2): 207-218.

546 Little D. N. Epps J. A. and Sebaaly P. E., 2006, The Benefits of Hydrated Lime in Hot Mix Asphalt,
547 National Lime Association.

548 Neville A.M. and Brooks J.J., 1987, *Concrete Technology*, Longman Scientific & Technical,
549 Longman Group UK Ltd. England.

550 Othman A.M., 2011, Evaluation of Hydrated Lime Effect on the Performance of Rubber-Modified
551 HMA Mixtures, *Journal of Elastomers and Plastics*, **43**: 221-237.

552 Satyakumar M., Chandran R. S. and Mahesh M. S., 2013, Influence of Mineral Fillers on the
553 Properties of Hot Mix Asphalt, *International Journal of Civil Engineering and Technology*, **4**: 99-
554 110.

555 SCRB/R9, 2003, General Specification for Roads and Bridges, Section R/9, Hot-Mix Asphalt
556 Concrete Pavement, Revised Edition. State Corporation of Roads and Bridges, Ministry of
557 Housing and Construction, Republic of Iraq.

558 Sebaaly P. E., Hilty E. and Weizel D., 2001, Effectiveness of Lime In Hot Mix Asphalt Pavement,
559 University of Nevada, Reno, USA.

560 Strategic Highway Research Program (SHRP), 1994, The Superpave Mix Design System, Manual
561 of Specifications, Tests Methods, and Practices, SHRP-A-379, National Research Council,
562 Washington, D. C., USA.

563 Southgate, H. Deen R., Havens J., Drake W., 1977, Kentucky Research: A Flexible Pavement
564 Design and Management System, Proceedings 4th International Conference on Structural Design
565 of Asphalt Pavements, Vol. II, the University of Michigan, Ann Arbor, Michigan, USA.

566 Witczak, M., 1972, Design of Full Depth Air Field Pavement, Proceedings, 3rd International
567 Conference on the Structural Design of Asphalt Pavements, London.

568

569

570

571

Table 1. Filler contents in the mixes for different applications.

Hydrated Lime Content (% in weight)	Wearing Course		Levelling Course		Base Course	
	Mixture*	Limestone Content (% in weight)	Mixture*	Limestone Content (% in weight)	Mixture*	Limestone Content (%in weight)
0	CW	7	CL	6	CB	5
1	H1W	6	H1L	5	H1B	4
1.5	H1.5W	5.5	H1.5L	4.5	H1.5B	3.5
2	H2W	5	H2L	4	H2B	3
2.5	H2.5W	4.5	H2.5L	3.5	H2.5B	2.5
3	H3W	4	H3L	3	H3B	2

572 * Mixture Nomenclature - C: control, W: Wearing, L: Levelling, B: Base, H: hydrated lime

573

574

575

576

Table 2. Aggregate Gradations of Asphalt Concrete Courses

Sieve Size		Wearing Course		Leveling (Binder) Course		Base Course	
inch	Mm	Selected grade % passing	Specification limits	Selected grade % passing	Specification limits	Selected grade % passing	Specification limits
1.5	37.0	-	-	-	-	100	100
1	25.0	-	-	100	100	95	90-100
$\frac{3}{4}$	19.0	100	100	95	90-100	83	76-90
$\frac{1}{2}$	12.5	95	90-100	80	70-90	68	56-80
$\frac{3}{8}$	9.5	83	76-90	69	56-80	61	48-74
No. 4	4.75	59	44-74	50	35-65	44	29-59
No. 8	2.36	37	28-58	35	23-49	32	19-45
No. 50	0.3	13	5-21	13	5-19	11	5-17
No. 200	0.075	7	4-10	6	3-9	5	2-8

577

578

Table 3. Traffic Information for Estimating the 80-kN ESAL

<ul style="list-style-type: none"> • Road: 2-lane road • Traffic Analysis Period = 15 years • Assumed current AADT = 2500 (during the first year) • Directional distribution factor = 50 % • Lane distribution factor = 100% • Percentage of Trucks = 45% • Annual growth rate = 4 % 					
Vehicle type	Percentage of <i>i</i> th vehicles P_i %	Number of vehicles/lane per year n_i	Equivalent Axle Load Factor EALF	Growth Factor G_f	ESALs
Passenger-vehicles (PCU)	55	250937.5	0.0008	20.02	4019.015
Single-unit trucks:					
2 axle, 4 tire	10	45625	0.003	20.02	2740.238
2 axle, 6 tire	10	45625	0.21	20.02	191816.6
3 axle or more	5	22812.58	0.61	20.02	278590.8
Tractor semitrailers and combinations:					
4-axle or less	5	22812.5	0.62	20.02	283157.9
5-axle	10	45625	1.09	20.02	995619.6
6-axle or more	5	22812.5	1.23	20.02	561748.7
Total	100	456250			2317693
The Estimated Design ESALs = 2.318×10^6					

582

583

Table 4. Parameters for the Modelled Resilient Modulus

Layer	Control Mix, 0% HL			Optimum Mix, 2.5% HL		
	a	b	c	a	B	c
Wearing	0.2819	-41.527	2089.7	0.1898	-43.033	2623
Leveling	0.3877	-46.413	1929.3	0.5248	-63.299	2526.7
Base	0.3404	-40.406	1649.3	0.3359	-41.117	1802.6

584

585

586

587

588

589

Table 5. Poisson Ratios for Different Paving Materials (Southgate et. al., 1977)

Material	Range	Typical Value
Asphalt concrete	0.30 - 0.40	0.35
Unstabilized granular subbase and base	0.30 - 0.45	0.4
Silty subgrade	0.35 - 0.45	0.45
Clay subgrade	0.4 – 0.5	0.5

590

591